Akalezi et al. International Journal of Industrial Chemistry 2012, 3:13
http://www.industchem.com/content/3/1/13

International Journal of Industrial Chemistry (IJIC)
a SpringerOpen Journal

RESEARCH Open Access

Application of aqueous extracts of coffee senna for control of mild steel corrosion in acidic environments

Chris O Akalezi, Conrad K Enenebaku and Emeka E Oguzie*

Abstract

Background: The inhibitive effect of the aqueous extract of *Coffee senna* (CS) on the corrosion of mild steel in 1 M HCl and 0.5 M H_2SO_4 solutions was investigated by weight loss measurement as well as potentiodynamic polarization and electrochemical impedance spectroscopy (EIS) measurements.

Result: The extract was found to efficiently inhibit the corrosion process in both environments and inhibition efficiency increased with extract concentration as well as rise in temperature. Data from electrochemical measurements suggest that the extract functioned by adsorption of the organic matter on the metal/corrodent interface, inhibiting both the anodic and cathodic half reactions of the corrosion process. Adsorption of the extract organic matter was approximated by the Langmuir isotherm. The adsorption behavior of selected organic constituents of the extract on the metal surface was assessed at the molecular level, in the framework of the density functional theory.

Conclusion: This study clearly shows the potentials of CS extract for control of mild steel corrosion in acidic environment.

Keywords: Coffee senna, Corrosion inhibition, Biomass extract, Mild steel, Density functional theory

Background

Iron and steel are the metallic materials most used in structures exposed to the atmosphere and often, to the aggressive environments in industrial applications due to their availability and low cost [1]. Acidic solutions are extensively used in acid cleaning, pickling, and descaling processes, as well as for drilling operations in oil and gas exploration [2]. Iron and steel surfaces deployed in service in these environments undergo considerable corrosion. Significant reduction in corrosion rates has been achieved by various means including reduction of the metal impurity content, application of several surface modification techniques as well as incorporation of suitable alloying elements. However, the use of corrosion inhibitors is about the most practical and economical methods for corrosion protection and prevention of unexpected metal dissolution in aqueous aggressive media [3-5]. A good number of the efficient corrosion inhibitors are organic compounds that contain nitrogen, oxygen, sulfur, phosphorus, and multiple bonds or aromatic rings in their structures [6-9]. The molecular electronic structures and electron densities around these functional groups are the key structural features that determine the effectiveness of inhibition [10-12].

The final choice of an appropriate inhibitor for a particular application is, however, constrained by such considerations as cost, environmental and toxicity issues (due to increasing concerns about the environment) as well as the vast variety of possible corrosion systems, which often necessitates the use of combinations of additives to provide the multiple services required for effective corrosion inhibition. Interestingly, extracts from natural products (biomass) contain several phytochemical constituents, including alkaloids, tannins, flavonoids, saponins, amino acids, ascorbic acid, phenolic acids, pigments resins, triterpenoids, which possess electronic structures akin to those of conventional organic corrosion inhibitors as described above. A number of such biomass extracts have actually been investigated for

* Correspondence: oguziemeka@yahoo.com
Electrochemical and Material Science Unit (EMRU), Department of Chemistry, Federal University of Technology Owerri, Imo State PMB 1526, Nigeria

corrosion inhibiting efficacy: The extracts of *Azadirachta indica*, fenugreek leaves, *Zanthoxylum alatum*, *Opuntia, Nypa fruticans, Ocimum viridis, Phyllanthus amarus*, chamomile, halfabar, and black cumin have been studied as corrosion inhibitors in hydrochloric and sulphuric acid media [13-21]. Zucchi and Omar [22] studied the corrosion inhibition of mild steel in hydrochloric acid solutions using aqueous extracts of papaya, *Poinciana pulcherrima, Cassia occidentalis* and *Datura stramonium* seeds. Gunasekaran and co-workers [23,24] studied the corrosion inhibition of steel by *Zanthoxylum alatum* extract in HCl as well as in phosphoric acid media. El-Etre studied the corrosion inhibition of copper, aluminum, zinc, and steel using natural honey as well as *Opuntia*, *Lawsonia*, and khillah extracts [25-27]. Oguzie and co-workers investigated the corrosion inhibiting effects of leaf extracts of *Telferia occidentalis* [28], *Azadirachta indica* [29], and *Hibiscus sabdariffa* [30] as well as extracts from the seeds of *Garcinia kola* [31] on mild steel corrosion in acidic solutions. Other than the biomass extracts, pure organic compounds extracted from natural products such as ascorbic acid [32], succinic acid [33], tryptamine [34], caffeine [35], Pennyroyal oil [36], amino acids [37], and caffeic acid [38,39] have also been evaluated as corrosion inhibitors. The results from these studies all confirm that biomass extracts possess remarkable abilities to inhibit the corrosion reaction.

The study of biomass extracts as metal corrosion inhibitors is beneficial for several reasons: they are inexpensive, readily available, nontoxic, and on the basis of their multi-constituent composition, could provide broad spectrum action (as opposed to the specificity of action of conventional organic inhibitors). These are attractive and desirable features for next generation corrosion inhibitors. Accordingly, the present report continues to focus on the broadening application of biomass extracts for metallic corrosion control and reports on the inhibiting effect of the leaf extract of coffee senna (CS) on the acid corrosion of mild steel. Coffee senna belongs to the family, Fabaceae, and is generally found in tropical and coastal plains of Africa and America. Extensive phytochemical characterization revealed that the plant is rich in anthraquinones, emodin glycosides, achrosine, chrysophanol, aloe-emodine, quercetine, rhamnosides, rhein, and vitexin alkaloids [40-42]. The plant is used in traditional medicine against throat inflammation, colds, asthma, fever, flu and as anti venom [43].

Corrosion inhibition efficiency has been experimentally evaluated using gravimetric, electrochemical impedance, and potentiodynamic polarization techniques. We have also analyzed the electronic and adsorption structures of some extract constituents with acquiescent molecular structures, within the framework of the density functional theory (DFT), to theoretically ascertain their possible adsorption modes and evaluate their individual contributions to the observed inhibiting effect.

Methods

Results and discussion

Weight loss measurements

The spontaneous dissolution of mild steel in 1 M HCl and 0.5 M H_2SO_4 in the presence of CS as corrosion inhibitor was studied by gravimetric measurements. Figure 1 presents the corrosion rate of the mild steel coupons in both acid media without and with different concentrations of CS 303 K. The plots show that the corrosion of the specimen was reduced with increasing extract concentration, i.e. the corrosion resistance was enhanced with increasing extract concentration. The weight loss data was used to calculate inhibition efficiency (IE%) of CS using the following equation:

$$\mathrm{IE}\% = \frac{wo - wi}{wo} \times 100 \qquad (1)$$

Where w_i and w_o are the weight losses in the presence and absence of extract respectively.

Figure 2 illustrates the variation of IE% with CS concentration in 1 M HCl and 0.5 M H_2SO_4 at 303 K. The plots reveal that IE% increased with increase in CS concentration. It is also obvious from the plots that the extract was slightly more effective in HCl solution at all concentrations, which can be explained on the basis of a cooperative adsorption mechanism involving chloride ions adsorbed on the metal surface [21,44]. This observation is justified by the fact that some of the extract species will be protonated in the acid solutions, and adsorption of such protonated species will be facilitated by the adsorbed chloride ions [45-50].

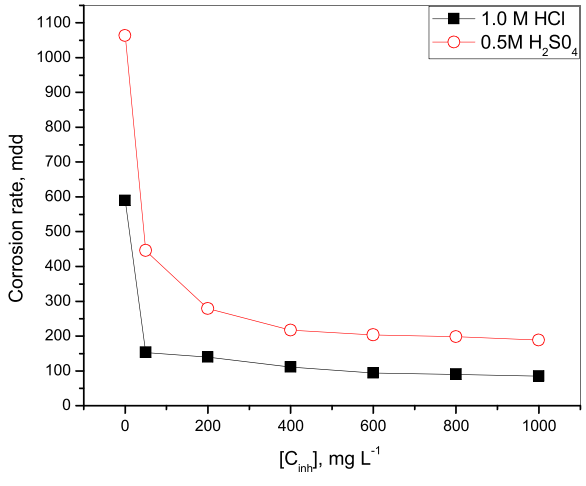

Figure 1 Effect of CS extract on the corrosion of mild steel at 303 K.

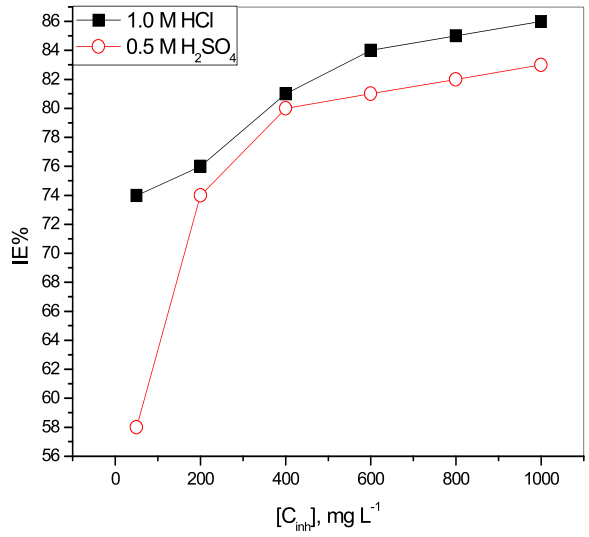

Figure 2 Inhibition efficiency of CS extracts in 1.0 M HCl and 0.5 M H_2SO_4 at 303 K.

In order to clarify the nature of adsorption, the gravimetric data in 1 M HCl and 0.5 M H_2SO_4 at 303 K were fitted to a series of adsorption isotherms including Frumkin, Langmuir, and Temkin isotherms and the best fit was obtained with the Langmuir isotherm:

$$C/\theta = 1/b + C \quad (2)$$

The corresponding linear plots of C/θ vs. *C* are presented in Figure 3 for CS adsorption from both 1 M HCl and 0.5 M H_2SO_4 (with slopes of 1.15 and 1.17 respectively), suggesting that the experimental data follows the Langmuir isotherm. The nonzero intercepts on the *y* axes and slopes ≠ 1.0 mean that some of the adsorbed species interact with each other and that the adsorption heat changes with increasing surface coverage.

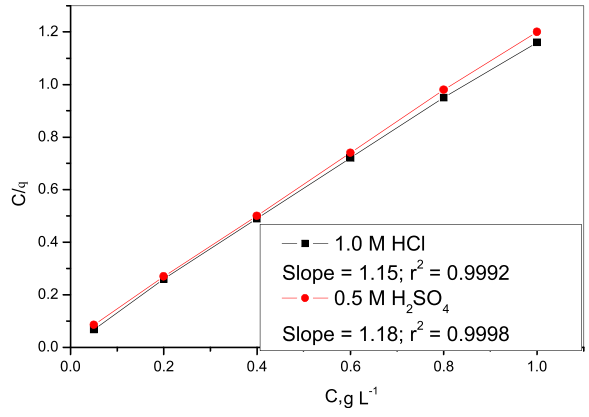

Figure 3 Langmuir isotherms for the adsorption of CS extract onto mild steel at 303 K.

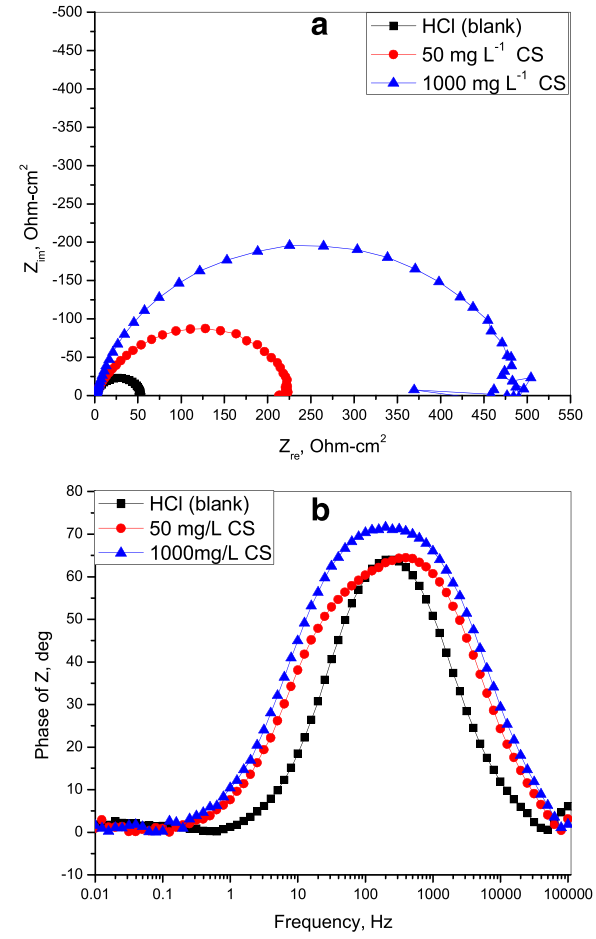

Figure 4 Electrochemical impedance spectra of mild steel in 1 M HCl solution. Electrochemical impedance spectra of mild steel in 1 M HCl solution without and with CS: (**a**) Nyquist and (**b**) Bode phase angle plots.

Electrochemical impedance spectroscopy measurements

In order to obtain information about the kinetics of interfacial mass transfer processes for mild steel corrosion in the presence of the extract, impedance measurements were undertaken in 1 M HCl and 0.5 M H_2SO_4 solutions without and with 50 mg L^{-1} and 1,000 mg L^{-1} CS. The recorded electrochemical impedance spectroscopy spectra in inhibited and uninhibited solutions are presented in the Nyquist and Bode phase angle formats in Figures 4 and 5 for 1 M HCl and 0.5 M H_2SO_4 solutions, respectively. The Nyquist plots all show one depressed capacitive loop, corresponding to only one maximum in the phase angle versus frequency; hence, a single time constant for the impedance response [51]. The transfer function can be represented by a solution resistance R_s, shorted by a capacitor (*C*) that is placed in parallel to the charge transfer resistance R_{ct} [20]:

$$Z_{(\omega)} = R_s + \left(\frac{1}{R_{ct}} + j\omega C\right)^{-1} \quad (3)$$

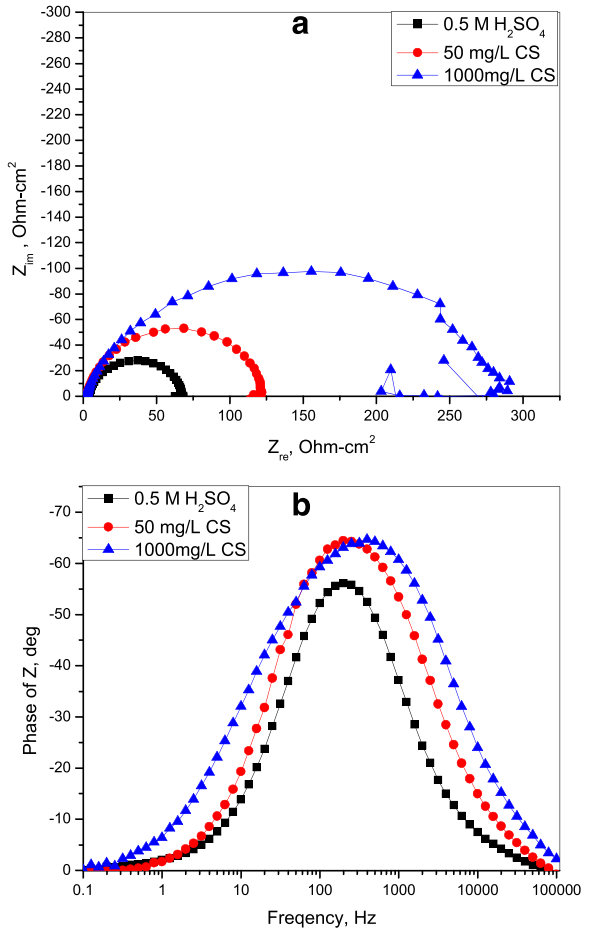

Figure 5 Electrochemical impedance spectra of mild steel in 0.5 M H_2SO_4 solution. Electrochemical impedance spectra of mild steel in 0.5 M H_2SO_4 solution without and with CS: (**a**) Nyquist and (**b**) Bode phase angle plots.

The observed depression of the capacitive loop, however, indicates frequency dispersion of interfacial impedance. This anomalous phenomenon is attributed to the nonhomogeneity of the electrode surface arising from the surface roughness or interfacial phenomena [4,52]. When such non-ideal frequency response is present, the capacitor is replaced by a constant phase element (CPE), with impedance Z_{CPE} as follows [19,20]:

$$Z_{CPE} = Q^{-1}(j\omega)^{-n} \tag{4}$$

Q and n stand for the CPE constant and exponent respectively; $j = (-1)^{1/2}$ is an imaginary number, ω is the angular frequency in radians s^{-1}, ($\omega = 2\pi f$) where f is the frequency in hertz. The double layer capacitance was calculated using the following equation:

$$C_{dl} = \frac{1}{2\pi f_{max}\, Rct} \tag{5}$$

where f_{max} is the frequency at which the imaginary component of impedance is maximum.

The impedance spectra for the Nyquist plots were appropriately analyzed by fitting into the equivalent circuit model $R_s(Q_{dl}R_{ct})$ (Figure 6). The corresponding electrochemical parameters given in Table 1 reveal that the charge transfer resistance values increased and the capacitance values decreased in the presence of CS extract. The increase in R_{ct} values including the corresponding increase in the magnitude of the phase angle peaks is attributed to the corrosion inhibiting effect of the extract. The decrease in C_{dl} values, which normally results from a decrease in the dielectric constant and/or an increase in the double-layer thickness, can be attributed to the adsorption of the extract organic matter onto the metal/electrolyte interface. These observations mean that the CS extract functioned as an adsorption-type inhibitor in both 1 M HCl and 0.5 M H_2SO_4.

The percentage inhibition efficiency (IE_R%) was calculated from the impedance data using the equation:

$$IE_R\% = \frac{R_{ct,inh} - R_{ct,bl}}{R_{ct,inh}} \times 100 \tag{6}$$

where $R_{ct,inh}$ and $R_{ct,bl}$ are charge transfer resistances in the presence and absence of CS extract. The obtained values presented in Table 1 follow the same trend with those obtained from weight loss measurements.

Potentiodynamic polarization measurements

Potentiodynamic polarization plots illustrating the effect of CS extract on the anodic and cathodic processes for mild steel corrosion in 1 M HCl and 0.5 M H_2SO_4 are shown in Figure 7a,b. The corresponding polarization parameters are presented in Table 2. A comparison of the potentiodynamic plots illustrate clearly that CS functioned by different mechanisms in the two acid media. Accordingly, CS functioned via a mixed inhibition mechanism in 1 M HCl, reducing the anodic and cathodic currents, with a slight shift of E_{corr} in the anodic direction. In 0.5 M H_2SO_4 on the other hand, a considerable

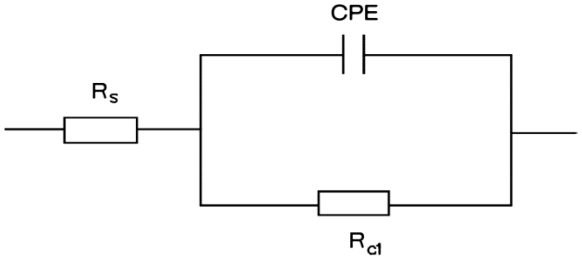

Figure 6 The electrochemical equivalent circuit used to fit the impedance spectra: *Rs*, solution resistance; R_{ct}, charge transfer resistance, CPE, constant phase element.

Table 1 Impedance parameters for mild steel corrosion without and with CS extract at 303 K

System	R_s (Ωcm^2)	R_{ct} (Ωcm^2)	C_{dl} (μFcm^{-2})	IE_R%
1.0 M HCl	1.32	94.03	77.09	
50 mg L^{-1} L CS	1.43	223.5	56.56	57.9
1,000 mg L^{-1} CS	1.43	481.9	41.60	80.5
0.5 M H_2SO_4	3.76	63.11	53.71	
50 mg L^{-1} CS	2.46	138.8	50.32	53.5
1000 mg L^{-1} CS	2.16	296.3	36.26	78.7

Table 2 Polarization parameters for mild steel corrosion without and with CS extract at 303 K

System	i_{corr} (μA cm^{-2})	E_{corr} (mV)	IE%
1.0 M HCl	354.66	−522	-
50 mg L^{-1} CS	206.85	−507	41.7
1000 mg L^{-1} CS	105.12	−485	70.4
0.5 M H_2SO_4	607.21	−482	-
50 mg L^{-1} CS	245.63	−509	56.42
1000 mg L^{-1} CS	151.73	−488	75.12

displacement of E_{corr} in the cathodic direction is observed and the cathodic reaction is significantly inhibited, which means that CS performed essentially as a cathodic inhibitor. As noted earlier [21,44], the ability of Cl^{-1} ions in the hydrochloric acid to be strongly adsorbed on the metal surface and hence, facilitate physical adsorption of inhibitor cations, is an important consideration towards the difference in mechanism of inhibition.

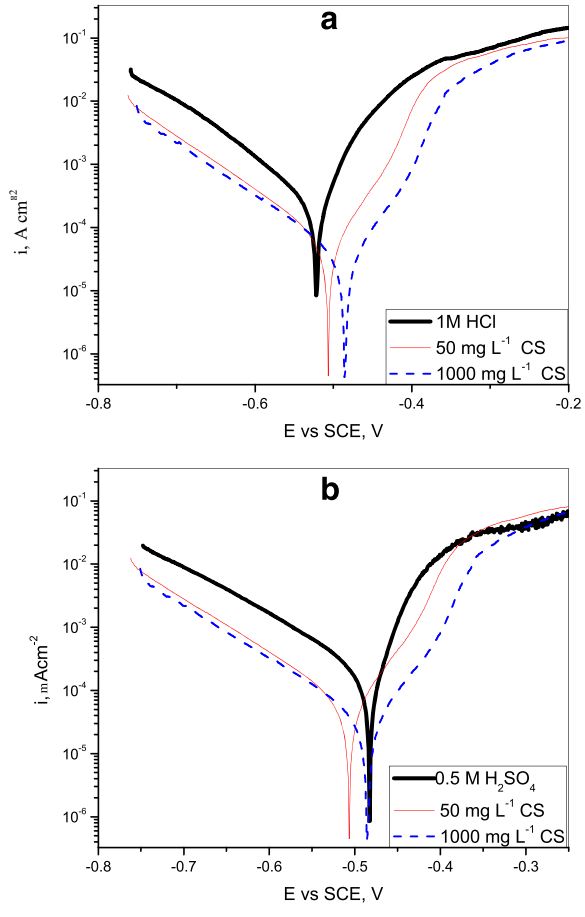

Figure 7 Potentiodynamic polarization curves of mild steel in (a) 1 M HCl and (b) 0.5 M H_2SO_4 solutions without and with CS extract.

The values of the corrosion current density in the absence ($i_{corr,bl}$) and presence of inhibitor ($i_{corr,inh}$) were used to estimate the inhibition efficiency from polarization data (IE_i%) as follows:

$$IE_i\% = \left(1 - \frac{i_{corr,inh}}{i_{corr,bl}}\right) \times 100 \quad (7)$$

($i_{corr,bl}$) and ($i_{corr,inh}$) are the corrosion current densities in the absence and presence of CS extract. The displayed data show that the addition of CS extract decreased the corrosion current density in both acid media. Also, it can be clearly seen that the inhibition efficiency increased with CS concentration, in agreement with the trends of the gravimetric and impedance data.

Effect of temperature

In order to understudy the temperature dependence of corrosion rates in uninhibited and inhibited solutions, gravimetric measurement were carried out in the temperature range 303–333 K in the absence and presence of 50 mg L^{-1} and 1,000 mg L^{-1} CS. The calculated values of the corrosion rates and inhibition efficiencies within the studied temperature range are shown in Table 3. Generally, the corrosion rates of mild steel in acidic solutions increase with the rise in temperature. This is due to a decrease in the overpotential of the hydrogen evolution reaction, resulting in higher dissolution rates of metals. The higher rate of hydrogen gas generation also increasingly agitates the metal

Table 3 Effect of temperature on weight loss and inhibition efficiency in 1.0 M HCl and 0.5 M H_2SO_4

System	313 K		323 K		333 K	
	C_R(mdd)	IE%	C_R(mdd)	IE%	C_R(mdd)	IE%
1.0 M HCl	846.9		2,756.3		15,000.8	
50 mg L^{-1} CS	239.7	71.7	649.0	76.5	1,063	92.9
1000 mg L^{-1} CS	197.9	76.64	367.4	86.7	593.1	96.4
0.5 M H_2SO_4	1,947.1		6,626.3		26,143.0	
50 mg L^{-1} CS	1,006.0	48.3	1,546.1	76.7	5,515.6	78.9
1000 mg L^{-1} CS	342.3	82.4	639.6	90.34	1,087.6	95.8

corrodent/interface and depending on the nature of the metal-inhibitor interactions, could as well hinder inhibitor adsorption or perturb already adsorbed inhibitor. On the other hand, for inhibitor species that react with the metal surface, increasing the temperature of the system could augment the interaction between the metal surface and the inhibitor leading to higher surface coverage. Inspection of the data in Table 3 shows that the corrosion rate of the mild steel specimen in all systems increased with temperature as expected. This effect is however notably subdued in inhibited solution, which means that CS extract maintains its inhibiting effect at higher temperature. Improved inhibitor adsorption at higher temperatures reflected by the trend of increasing inhibition efficiency with rise in temperature is an indication that some of the extract components become well adsorbed (chemisorbed) at higher temperature and so contribute more to the overall inhibiting effect.

The dependence of corrosion rate on temperature can be expressed by the Arrhenius equation [53,54]:

$$\log C_{R=} \frac{-E_a}{2.303RT} + A \qquad (8)$$

where E_a is the apparent effective activation energy, R the general gas constant and A the Arrhenius pre-exponential factor. A plot of the logarithm of the corrosion rate, (C_R) vs. 1/T gave a straight line as shown in Figure 8, with slope of $-E_a/2.303$ R. The calculated activation energies for the corrosion process in 1 M HCl was found to be 63.35 kJ mol^{-1}, and the values obtained in the presence of 50 and 1,000 mg L^{-1} CS were 29.65 and 37.59 kJ mol^{-1}, respectively. Similarly, E_a in 0.5 M H_2SO_4 was 65.15, 46.15, and 33.19 kJ mol^{-1} for uninhibited and inhibited solutions containing 50 mg L^{-1} and 1,000 mg L^{-1} CS, respectively. CS extract thus reduces the corrosion activation energies for mild steel in 1 M HCl and 0.5 M H_2SO_4. This means that the extract is more effective at higher temperature [55-58] and confirms our previous assumption that chemisorption of some constituents of the extract becomes more pronounced at higher temperatures. This is because unchanged or lowered activation energies in inhibited solutions may be interpreted as being indicative of chemisorption, while the opposite is the case with physical adsorption [59,60].

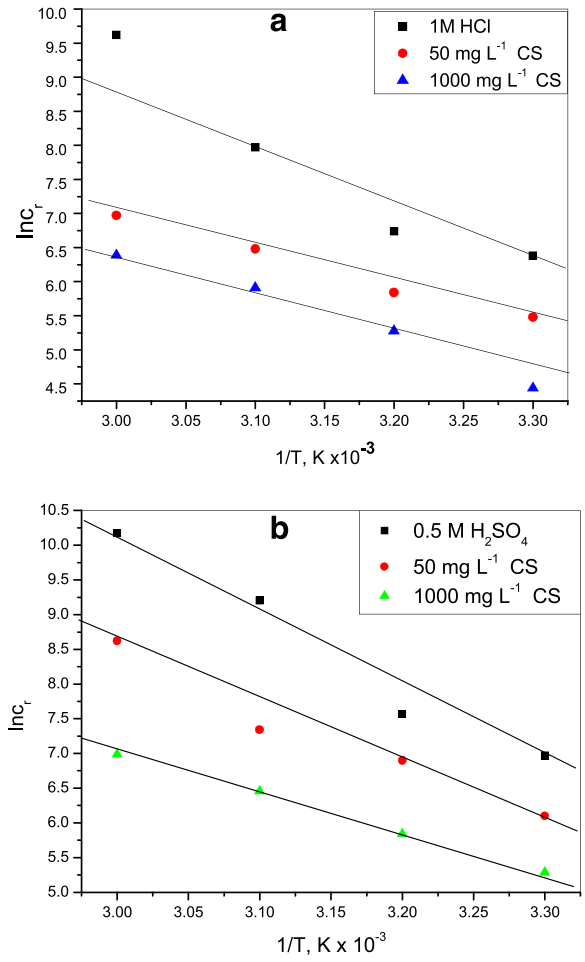

Figure 8 Arrhenius plots for mild steel corrosion in (a) 1 M HCl and (b) 0.5 M H_2SO_4 without and with CS extract.

Quantum chemical calculations

Our experimental results indicate that CS extract functions as an adsorption-type corrosion inhibitor. The complex processes associated with metal-inhibitor interactions can be theoretically investigated at the molecular level using computer simulations of suitable models in the framework of the density functional theory (DFT). Recently, we have extended the application of DFT techniques to the assessment of the adsorption behavior of selected constituents of biomass extracts, especially those with molecular structures similar to conventional corrosion inhibitors [61]. Such quantum chemical computations are not necessarily intended to provide a detailed description of the adsorption of the extract. Instead, the idea is to recognize the relative contributions of the different extract components through their individual adsorption strengths and mechanisms. The main constituents of CS extract chosen for the computations include anthraquinone (ATQ), emodine (EMD), chrysophanol (CRP), aloe-emodine (ALE), and rhein (RH). The molecules are all derivatives of anthraquinone, and hence have the same molecular backbone.

The first consideration was to assess the electronic structures of the molecules, including the distribution of frontier molecular orbitals and Fukui indices, with a view to establish the active sites as well as local reactivity of the molecules. The simulations were performed by

means of the DFT electronic structure program DMol3 available in Material Studio 4.0 (Accelrys Inc., San Diego, CA, USA) [62-65] Electronic parameters for the simulation include restricted spin polarization using the DND basis set and the Perdew-Wang local-correlation-density functional. The molecular structures were initially subjected to geometry optimization using the COMPASS force field (Accelrys Inc., San Diego, CA, USA). Figure 9 illustrates the highest occupied molecular orbital (HOMO), lowest unoccupied molecular orbital (LUMO), as well as the total electron density of ATQ, EMD, CRP, ALE, and RH; while the corresponding quantum chemical parameters are presented in Table 4. Interestingly, the HOMO-LUMO locations are actually almost identical for all the molecules, which could lead to some similarities in their adsorption characteristics.

The region of highest electron density, HOMO, are the sites at which electrophiles attack and represents the

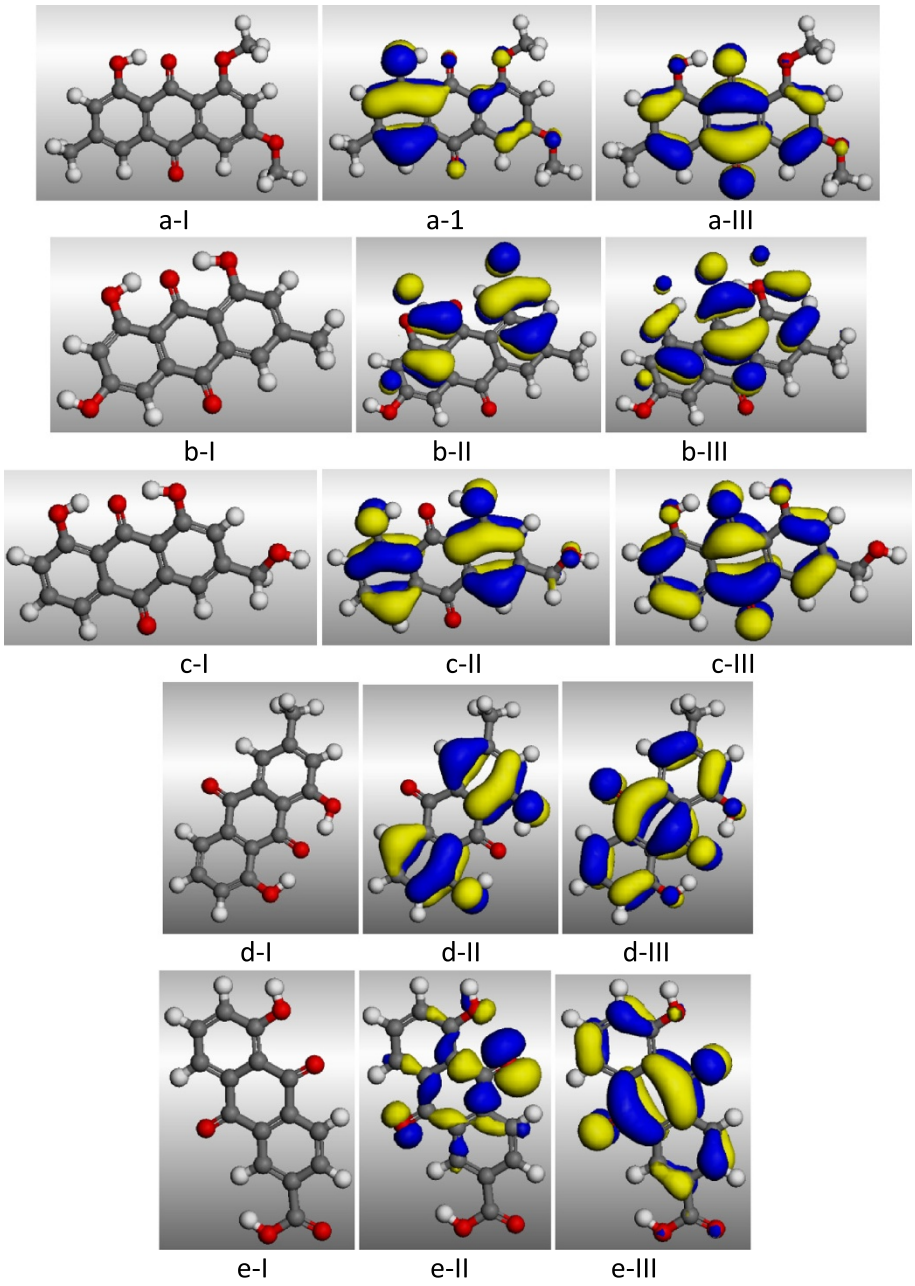

Figure 9 Electronic properties of a, ATQ; b, EMD; c, ALE; d, CRP; e, RH: [I, optimized structures; II, HOMO orbitals; III, LUMO orbital]. Atom legend: gray, C; white, H; red, O. The blue and yellow isosurfaces depict the electron density difference; the blue regions show electron accumulation, while the yellow regions show electron loss.

Table 4 Calculated quantum chemical properties for the most stable conformation of the major phytochemical constituents of CS extract

Compound	E_{HOMO} (eV)	E_{LUMO} (eV)	ΔE (eV)	μ (Debye)	E_{bind} (kcalmol^{-1})
ATQ(298)	−5.576	−3.664	1.911	3.532	−183.40
EMD(170)	−5.892	−3.939	1.953	0.580	−155.0
CRP(154)	−5.991	−4.041	1.950	1.400	−136.10
ALE(154)	−5.934	−3.997	1.134	2.906	−136.62
RH(184)	−6.610	−4.543	2.067	1.905	−146.90

active sites with the utmost ability to bond to the metal surface, whereas the LUMO orbital can accept electrons from the 3d orbital of the Fe atom to form feedback bonds. The HOMO energy (E_{HOMO}) expresses the intrinsic electron donating tendency to an appropriate acceptor i.e., any molecule with lower HOMO energy and empty molecular orbital; while the energy of LUMO (E_{LUMO}) is directly related to the electron affinity and characterizes the susceptibility of the molecule toward attack by nucleophiles [66-68]. Low values of the gap ($\Delta E = E_{LUMO} - {}_{HOMO}$), will render good inhibition efficiencies since the energy to remove an electron from the last occupied orbital will be minimized.

The E_{HOMO} and E_{LUMO} values do not vary very significantly for all the molecules, probably because the functional groups that comprise their HOMO and LUMO locations are comparable. The ΔE values again do not vary so much which means that any observed differences in their adsorption strengths would result from molecular size parameters rather than electronic structure parameters. The seemingly low values of ΔE (approximately 2 eV) suggest that interaction of the molecules with the metal surface would likely involve electron transfer processes.

Molecular dynamics simulation

The adsorption of the different molecules on the metal surface was analyzed at a molecular level by molecular dynamics simulations, using Forcite quench molecular dynamics to sample many different low energy configurations and identify the low energy minima [69,70]. Among the different steps involved in the modeling approach was the construction of the iron surface from the pure crystal. The surface consists of Fe slab with dimensions ($10 \times 12 \times 3$ Å) with periodic boundary conditions devoid of any arbitrary effects. The Fe slab was first cleaved along the (110) plane with the uppermost and lowest layers fixed. The molecules were adsorbed on one side of the slab. Temperature was fixed at 303 K, with fixed number-volume-energy (microcanonical) ensemble, with a time step of 1 fs and simulation time 5 ps. The system was quenched every 250 steps. Optimized structures of ATQ, EMD, CRP, ALE, and RH were used for the simulation. We have neglected solvent and charge effects in all our simulations and performed the calculations at the metal/vacuum interface. Although this is clearly an oversimplification of the actual situation, it is adequate to qualitatively illustrate the differences in the adsorption behavior of the molecules and provide sufficient insight for our study objectives.

Figure 10 shows representative snapshots of the cross-section of the lowest energy adsorption configurations for the single molecules on the Fe (110) surface from our simulations. The molecules can be seen to maintain a flat-lying adsorption orientation on the Fe surface, in order to maximize contact and enhance the degree of surface coverage. This parallel adsorption orientation also facilitates interaction of π – electrons of the anthraquinone nucleus and the hetero-atoms with the metal surface. The binding energy (E_{bind}) between the iron surface and the inhibitor molecules was calculated as follows [69,70]:

$$E_{Bind} = E_{total} - (E_{mol} + E_{Fe}) \quad (9)$$

E_{mol}, E_{Fe} and E_{total} correspond respectively to the total energies of the molecule, Fe (110) slab and the adsorbed Mol/Fe (110) couple, where a negative value of E_{Bind} corresponds to a stable adsorption structure. The obtained values are given in Table 4. In each case the potential energies were calculated by averaging the energies of the five structures of lowest energy. As can be seen from the data, the binding energies are all negative and of considerable magnitude, suggesting stable adsorption structures. Again, the obtained values are of the same order of magnitude, in agreement with the trend of electronic structure properties from the quantum chemical computations.

The magnitude of the binding energies is actually in the range of chemisorptive interactions (>100 kcal mol^{-1}); this is despite the fact that our simulations did not take into consideration the specific (covalent) interactions between the molecules and the Fe surface, which means that the phytochemical constituents of CS extract are very strongly adsorbed on the mild steel surface. This observation can be related to the remarkable corrosion inhibition efficiency of the extract observed experimentally. Unraveling the basis for this behavior requires a more rigorous assessment of the output from the molecular dynamics simulations. A detailed analysis of the on-top view of the adsorbed molecules on Fe (110), as presented in Figure 11 for RH and CRP, reveals a very clear trend in the adsorption configuration in which polarizable atoms along the molecular backbone appear to align with vacant sites on the face-centered cubic lattice atop the metal surface. In other words, the anthraquinone nucleus seems to avoid contact with the Fe atoms on the surface

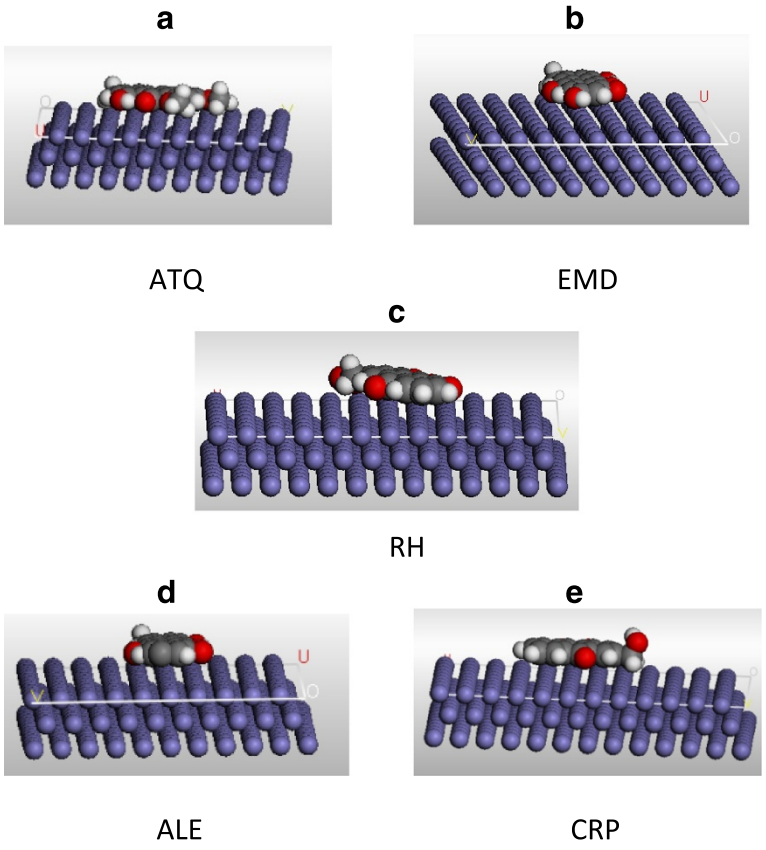

Figure 10 Perspective view of representative snapshots of molecular dynamics models (a) ATQ, (b) EMD, (c) RH, (d) ALE and (e) CRP adsorbed on Fe (110).

plane (larger spheres on the Fe slab) and is preferentially accommodated in characteristic epitaxial grooves on the metal surface. Such epitaxial adsorption configuration, which is associated with a minimum free energy of adsorption, has also been reported for some biochemical compounds (amino acids, peptides, etc.) [71,72] and accounts for the remarkably stable adsorption structures.

Methods

Materials preparation

Corrosion experiments were performed on mild steel specimens with weight percentage composition as follows; C, 0.05; Mn, 0.6; P, 0.36; Si, 0.3; and the balance Fe. The aggressive solutions were 1 M HCl and 0.5 M H_2SO_4 respectively, prepared from analytical grade

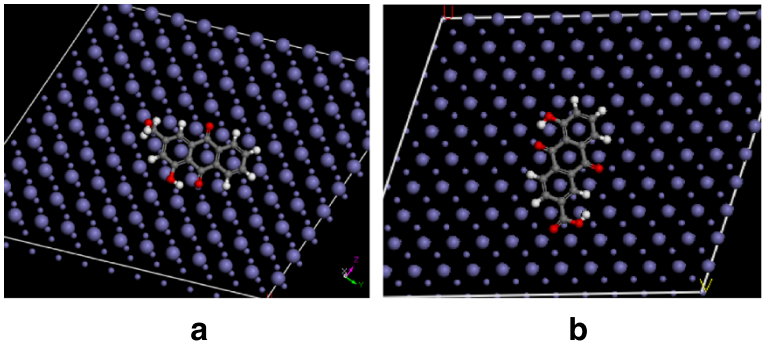

Figure 11 On-top views of representative snapshots from molecular dynamics models of (a) ALE and (b) RH adsorption on Fe (110), emphasizing the soft epitaxial adsorption mechanism with accommodation of the molecular backbone in characteristic epitaxial grooves on the Fe (110) slab.

reagents. Stock solutions of CS extract were prepared by boiling weighed amounts of dried and ground leaves of CS in 1 M HCl and 0.5 M H_2SO_4 solutions, respectively, under reflux for 3 h. The resulting solutions were cooled then triple-filtered. The amount of plant material extracted into the solution was quantified by comparing the weight of the dried residue with the initial weight of the dried plant material before extraction. From the respective stock solutions, inhibitor test solutions were prepared in the desired concentration range by diluting with the corresponding aggressive solution.

Gravimetric measurements

Gravimetric experiments were conducted on test coupons of dimension $3 \times 3 \times 0.14$ cm. Before each experiment, the coupons were abraded using emery papers (grades 200–1000) washed with distilled water and dried in acetone and warm air. The coupons were then weighed and suspended in beakers containing the test solutions using glass hooks and rods. Tests were conducted under total immersion conditions in 300 ml of the aerated and unstirred test solutions. The coupons were retrieved after 3 h, immersed in 20% NaOH solution containing 200 $g\,l^{-1}$ of zinc dust, scrubbed with bristle brush under running water, dried and reweighed. The weight loss was taken as the difference between the initial and final weights of the coupons. All tests were run in triplicate, and the data showed good reproducibility with standard deviation ranging from 0 to 0.00065. Average values for each experiment were obtained and used in subsequent calculations.

Electrochemical measurements

Metal samples for electrochemical experiments were of dimensions 1.5×1.5 cm. These were subsequently sealed with epoxy resin in such a way that only one square surface of area, 1.0 cm^2, was left uncovered. The exposed surface was degreased in acetone, rinsed with distilled water, and dried in warm air. Electrochemical experiments were conducted in a conventional three-electrode cell using a VERSASTAT 400 Complete DC Voltammetry and Corrosion System, with V3 Studio software (Advance Tech Inc., Andheri East, Mumbai, India). A platinum foil was used as counter electrode and a saturated calomel electrode (SCE) as reference electrode. The latter was connected via Luggin's capillary. Measurements were performed in aerated and unstirred solutions at the end of 1 h of immersion at 303 K. Impedance measurements were made at corrosion potentials (E_{corr}) over a frequency range of 100 kHz–10 mHz, with a signal amplitude perturbation of 5 mV. Potentiodynamic polarization studies were carried out in the potential range ±350 mV vs. corrosion potential at a scan rate of $0.33 mV s^{-1}$. Each test was run in triplicate to verify the reproducibility of the data.

Conclusions

The studied aqueous extract of CS leaves inhibited the corrosion of mild steel in 1 M HCl and 0.5 M H_2SO_4. The inhibition efficiency increased with the increase in concentration and with increase in temperature up to 333 K. Impedance results revealed that the extract functioned via adsorption of the organic matter on the metal/solution interface. The adsorption behavior as approximated by the Langmuir isotherm. Polarization measurements show that the adsorbed extract organic matter inhibited the corrosion process via mixed inhibition mechanism, affecting both the anodic metal dissolution reaction and the cathodic hydrogen evolution reaction. DFT-based quantum chemical computations of parameters associated with the electronic structures of specific components of the extract confirmed their inhibiting potential, which was further corroborated by molecular dynamics modeling of the adsorption of the single molecules on the metal surface.

Competing interests

The authors declare that she has no competing interests.

Authors' contributions

Enenebeaku, CK carried out the gravimetric measurements. Akalezi CO carried out the electrochemical measurements and drafted the manuscript. Oguzie, EE carried out the theoretical and participated in sequence alignment. All authors read and approved the manuscript.

Authors' information

Emeka Oguzie (PhD) is presently a Reader in the Department of Chemistry, Federal University of Technology Owerri and the Coordinator of the Electrochemistry and Materials Science Research Unit (EMRU). He holds a BSc (Hons) degree in Pure Chemistry from the University of Nigeria Nsukka, MSc in Analytical Chemistry from the Federal University of Technology Owerri and a PhD in Physical Chemistry from the University of Calabar. He was a visiting (CAS-TWAS) postdoctoral research fellow at the State Key Laboratory for Corrosion and Protection, Institute of Metal Research, Chinese Academy of Sciences, Shenyang, China. His research interests include the study of metal corrosion inhibition by organic dyes and plant extracts, membrane transport and biosorption processes. He has over 40 publications in international journals and has presented several papers at national and international conferences. He belongs to various professional associations and has recently been appointed an affiliate fellow of TWAS, the Academy of Sciences for the Developing World. His name is cited in Marquis Who's Who in Science and Engineering, 19th ed.(2006-2007) and in the Top 100 Scientists 2007 by International Biographical Centre, Cambridge, England. Emeka Oguzie is the corresponding author and can be contacted at: oguziemeka@yahoo.com Chris Akalezi is a Lecturer in the Department of Chemistry, Federal University of Technology Owerri, attached to the Physical Chemistry Section. He obtained his BSc in Industrial Chemistry from the Federal University of Technology Owerri, MSc in Physical Chemistry from the University of Lagos. He quit a fruitful career in the industry to join the academia and has ample industrial working experience. His research interest is in the area of surface coatings and corrosion inhibitors for oil and gas installations, which forms the basis of his proposed PhD research. He is a member of the Chemical Society of Nigeria and the American Chemical Society. Conrad Enenebeaku (PhD) is currently a Lecturer in the Physical Chemistry Section, Department of Chemistry, Federal University of Technology Owerri. He obtained his BSc in Pure Chemistry and MSc in

Applied Physical Chemistry from the University of Jos and PhD from the Federal University of Technology Owerri. He also holds another MSc in Computer Science from the University of Lagos and has extensive industrial working experience. He is a member of the Chemical Society of Nigeria and of the Institute of Chartered Chemists of Nigeria.

Acknowledgment
This project is supported by TWAS, the academy of Science for the developing world, under the TWAS Grants for Research units (TWAS-RGA08-005).

Received: 24 February 2012 Accepted: 5 May 2012
Published: 16 July 2012

References

1. Bentis F, Lagrence M, Traisnel M (2002) 2,5-bis(n-pyridyl)-1,3,4-oxadizoles as corrosion inhibitors for mild steel in acidic media. Corros Sci 56:733–742
2. Bothi RP, Sethuraman MG (2008) Natural products as corrosion inhibitors for metals in corrosive media- a review. Mater Lett 62:113–116
3. Satapathy AK, Gunasekaran G, Sahoo SC, Amit K, Rodrigues PV (2009) Corrosion inhibition by justicia gendarussa plant extract in hydrochloric acid solution". Corros Sci 51:2848–2856
4. De-Souza FS, Spinelli A (2009) Caffeic acid as a green corrosion inhibitor for mild steel. Corros Sci 52:1845
5. Da Rocha JC, Gomes DCP, D'Elia E (2010) "Corrosion inhibition of carbon steel in hydrochloric solution by fruit peel aqueous extracts. Corros Sci 52:2341–2348
6. Jia-Jun F, Li S-n, Wang Y, Cao L-H, Lu-de L (2010) Computational and electrochemical studies of some amino acid compounds as corrosion inhibitors for mild steel in hydrochloric acid solution. J Mater Sci 46:6255–6265
7. Shukla SK, Singh AK, Ahamad I, Quraishi MA (2009) Streptomycin: A commercially available drug as corrosion inhibitor for mild steel in hydrochloric acid. Mater Lett 63:819–822
8. Shukla SK, Quraishi MA (2009) Ceftriaxone: A novel corrosion inhibitor for mild steel in hydrochloric acid. J Appl Electrochem 39:1517–1523
9. Sinko J (2001) Challenges of chromate inhibitor pigments replacement in organic coatings. Prog Org Coat 42:267–282
10. Bothi RP, Sethuraman MG (2008) Inhibitive effect of black pepper extract on the sulphuric acid corrosion of mild steel. Mater Lett 62:2977–2979
11. Ketsetzi A, Stathoulopoulou A, Demadis KD (2008) Being "green" in chemical water treatment technologies: Issues, challenges and developments. Desalination 223:487–493
12. Umoren SA, Obot IB, Obi-Egbedi NO (2009) Raphia hookeri gum as a potential eco-friendly inhibitor for mild steel in sulphuric acid. J Mater Sci 44(1):274–279
13. Hackerman N, Hurd RM (1962) Proceedings of International Congress of Metallic Corrosion. Butterworth, London, p 166
14. Srivastava K, Srivastava P (1981) Studies on plant materials as corrosion inhibitors. Br Corros J 16(4):221–223
15. Valek L, Martinez S (2007) Mater Lett 61:148–151
16. Noor EA (2008) Comparative study on the corrosion inhibition of mild steel by aqueous extract of Fenugreek seeds and leaves in acidic solution. J Eng Appl Sci 3:23–30
17. Orubite KO, Oforka NC (2004) Inhibition of corrosion of mild steel in HCl solutions by the extracts of leaves of Nypa fruticans' wurmb. Mater Lett 58:1768–1772
18. Okafor PC, Ikpi ME, Uwah IE, Ebenso EE, Ekpe UJ, Umorem SA (2008) Inhibitory action of Phyllantus amaratus extracts on the corrosion of mild steel in acidic media. Corros Sci 50:2310–2317
19. Abdel-Gaber AM, Abd-El-Nabey BA, Sidahmed IM, El-Zayady AM, Saadawy M (2006) Inhibitive action of some plant extracts on the corrosion of steel in acidic media. Corros Sci 48:2765–2779
20. Abdel-Gaber AM, Abd-El-Nabey BA, Saadawy M (2009) "The role of acid anion on the inhibition of the acidic corrosion of steel by Lupin extract". Corrosion Science 51:1038
21. Jain BC, Gour JN (1978) Journal of Electrochemical Society of India 27:165
22. Zucchi F, Omar IH (1995) Plant Extracts as Corrosion Inhibitors of Mild Steel in HCl solution. Surface Technology 24:391–399
23. Chauhan LR, Gunasekaran G (2007) Corrosion inhibition of mild steel by plant extract in dilute HCl medium. Corros Sci 49:1143
24. Gunasekaran G, Chauhan LR (2004) "Eco friendly inhibitor for corrosion inhibition of mild steel in phosphoric acid medium", Electrochim. Acta 49:4387
25. El-Etre AY (1998) Natural honey as corrosion inhibitor. Corros Sci 40:1845
26. El-Etre AY (2003) Inhibition of aluminium corrosion using opuntia extract. Corros Sci 45:2485
27. El-Etre AY, Abdallah M, El-Tantawy ZE (2005) Corrosion inhibition of some metals using lawsonia extract. Corros Sci 47:385–395
28. Oguzie EE (2005) Inhibition of acid corrosion of mild steel by *Talfaria occidentalis* extract. Pigment Resin Technology 34(6):321–326
29. Oguzie EE (2005) Adsorption and corrosion inhibitive properties of *Azadirachta indica* in acid solutions. Pigment and Resin Technology 35:334–340
30. Oguzie EE (2008) Corrosion Inhibitive Effect and Adsorption Behaviour of *Hibiscus Sabdariffa* Extract on Mild Steel in Acidic Media. Portugese Electrochim Acta 26:303–314
31. Oguzie EE, Iyeh KI, Onuchukwu AI (2006) "Inhibition of mild steel corrosion in acidic media by aqueous extract from Garcinia kola seed". Bull Electrochem 22:63
32. El-Etre AY (2006) Khillar extact as inhibitor for cid corrosion of SX 316 steel. Appl Surf Sci 252:8521–8525
33. Oguzie EE (2008) Evaluation of the inhibitive effect of some plant extracts on the acid corrosion of mild steel. Corros Sci 50:2993
34. Gonçalves RS, Mello LD (2001) Electrochemical investigation of ascorbic acid adsorption on low-carbon steel in 0.5 M Na_2SO_4 solutions. Corros Sci 43:457
35. Amin MA, El-Rehim SSA, El-Sherbini EEF, Bayoumy RS (2007) The inhibition of low carbon steel corrosion in hydrochloric acid solutions by succinic acid: Part I. Weight loss, polarization, EIS, PZC, EDX and SEM studies. Electrochim Acta 52:3588
36. Moretti G, Guidi F, Grion G (2004) Tryptamine as a green iron corrosion inhibitor in 0.5 M deaerated sulphuric acid. Corros Sci 46:387
37. Fallavena T, Antonow M, Gonçalves RS (2006) "Caffeine as non-toxic corrosion inhibitor for copper in aqueous solutions of potassium nitrate. Appl Surface Science 253:566
38. Bouyanzer A, Hammouti B, Majidi L (2006) Pennyroyal oil from Mentha pulegium as corrosion inhibitor for steel in 1 M HCl. Material Letters 60:2840
39. Zhang DQ, Cai QR, Gao LX, Lee KY (2008) Effect of serine, threonine and glutamic acid on the corrosion of copper in aerated hydrochloric acid. Corros Sci 50:3615
40. Chukwujekwu JC, Coombes PH, Mulholland DA, Van Taden J (2006) "South African journal of Botany" 72(2):295–297
41. Li SF, Di YT, Wang Y-H, Tan C-J, Fang X, Yu Z, Zheng Y-T, Ling L, He H-P, Li S-L, Hao H-J (2010) Helvetica Chimica Acta 93(9):1795–1802
42. Hatano T, Mizuta S, Ito H, Yoshida T (1998) Phytochemistry 52(7):1379–1383
43. Yadav JP, Arya V, Yadav S, Panghal S, Kumarand S, Dhankhar S (2010) *"Cassia occidentalis* L.: A review on its ethnobotany, phytochemical and pharmacological profile". Fitoterapia 81(4):223–230. doi:10.1016/j.fitote.2009.09.008
44. Rosliza R, Wan Nik WB (2010) Improvement of corrosion resistance of AA6061 alloy by tapioca starch in seawater. Curr Appl Phys 10:221–229
45. Li X, Deng S, Fu H, Mu G, Zhoa N (2008) Synergism between rare earth cerium(IV) ion and vanillin on the corrosion of steel in H2SO4 solution: Weight loss, electrochemical, UV–vis, FTIR, XPS, and AFM approaches. Appl Surf Sci 254:5574–5586
46. Oguzie EE, Njoku VO, Enenebeaku CK, Akalezi CO, Obi C (2008) "Effect of hexamethylpararosaniline chloride (crystal violet) on mild steel corrosion in acidic media". Corros Sci 50:3480–3486
47. Quaraishi MA, Singh A, Sigh VK, Yadav DK, Sigh AK (2010) "Green Corrosion inhibitors of mild steel in hydrochloric acid and sulphuric acid solutions by the extract of Murraya koenigii leaves". Mater Chem Phys 122:114–122
48. Quaraishi MA, Khan S (2005) Thiadiazoles-A potential class of heterocyclic inhibitor for prevention of mild steel corrosion in hydrochloric acid solution. Indian J Chem Technol 12:576
49. Brelin CB, Carrol WM (1993) The activation of aluminium by indiumions in chloride, bromide and iodide solutions. Corros Sci 34:327–341
50. Khedr MGA, Lashien MS (1992) The role of metal cations in the corrosion and corrosion inhibition of aluminium in aqueous solutions. Corros Sci 33:137–151

51. Flis J, Zakroczymski T (1996) Impedance Study of Reinforcing Steel in Simulated Pore Solution with Tannin. J Electrochem Soc 143:2458
52. Ozcan M, Solmaz R, Kardas G, Dehri I (2008) Adsorption properties of barbiturates as green corrosion inhibitors of mild steel in phosphoric acid. Colloids Surf, A Physicochem Eng Asp 325:57–63
53. Khaled KF, Babic-Samardzija K, Hackerman N (2005) Theoretical study of the structural effects of polymethylene amines on corrosion inhibition of iron in acid solutions. Electrochim Acta 50:2515
54. Cheng S, Chen S, Liu T, Chang X, Yin Y (2007) Carboxymenthylchitosan as an eco-friendly inhibitor for mild steel in 1 M HCl. Mater Lett 61:3279
55. Putilover IN, Balezine SA, Baranik UP (1960) Metallic Corrosion inhibitors. Pergamon press, New York
56. CardozodaRocha J, AntôniodaCunha P, ElianeD'Elia E (2010) "Corrosion inhibition of carbon steel in hydrochloric acid solution by fruit peel aqueous extracts". Corrosion Sci 52:2341–2348
57. Martinez S, Stern I (2001) Inhibitory mechanism of low-carbon steel corrosion by mimosa tannin in sulphuric acid solutions". J Appl Electrochem 31:973–978
58. Popova A, Sokolova E, Raicheva S, Christov M (2003) "AC and DC study of the temperature effect on the mild steel corrosion in acid media in the presence of benzimidazole derivatives". Corrosion Science 45:33–58
59. Prabhu RA, Venkatesha TV, Shanbhag AV, Praveen BM, Kulkarni GM, Kalkhambkar RG (2008) Quinol-2-thione compounds as corrosion inhibitors for mild steel in acid solution. Mater Chem Phys 108:283–289
60. Tebbji K, Hammouti B, Oudda H, Ramdai A, Benkadour M (2005) Appl Surf Sci 252:1378
61. Oguzie EE, Enenebeaku CK, Akalezi CO, Okoro SC, Ayuk AA, Ejike EN (2010) Adsorption and corrosion-inhibiting effect of Dacryodis edulis extract on low-carbon-steel corrosion in acidic media *J*. Colloid & Interface Science 349:283–292
62. Delley B (1990) An All-Electron Numerical Method for Solving the Local Density Functional for Polyatomic Molecules. J Chem Phys 92:508–517
63. Delley B (2000) From molecules to solids with the DMol3 approach. J Chem Phys 113:7756–7764
64. Xia S, Qji M, Yu L, Liu P, Zhao H H (2008) Corros Sci 50:2021–2029
65. Khaled KF (2010) Corrosion of copper in nitric acid solutions using some amino acids: A **combined experimental and theoretical study**. Corros Sci 52:3225–3234
66. Rodriguez-Valdez LM, Martinez-Villafane A, Martinez L, Glossman-Mitnik D (2005) Corros Sci 716:61–65
67. Martinez S, Stagljar I (2003) "Correlation between the molecular structure and the corrosion inhibition efficiency of Chestnut tannin in acidic solutions". J Molecular structure (Theochem) 640:167–174
68. Chi M, Zhao Y-P (2009) Adsorption of Formaldehyde molecule on the intrinsic and Al-doped grapheme: A first principle study. Comput Mater Sci 48:1085–1090
69. Casewit CJ, Colwell KS, Rappé AK (1992) Application of a universal force field to organic molecules. J Am Chem Soc 114:10035–10046
70. Casewit CJ, Colwell KS, Rappé AK (1992) Application of a universal force field to main group compounds. J Am Chem Soc 114:10046–10053
71. Heinz H, Farmer BL, Pandey RB, Slocik JM, Patnaik SS, Pachter R, Naik RR (2009) Journal of American Chemical Society 131:9704–9714
72. Feng J, Pandey RB, Berry RJ, Farmer BL, Naik RR, Heinz H (2010) Adsorption mechanism of single amino acid and surfactant molecules to Au{111} surfaces in aqueous solutions: design rules for metal-binding molecules. Soft Matter. doi:10.1039/c0sm01118e

doi:10.1186/2228-5547-3-13
Cite this article as: Akalezi *et al.*: Application of aqueous extracts of coffee senna for control of mild steel corrosion in acidic environments. *International Journal of Industrial Chemistry* 2012 **3**:13.